Crustal Deformation Associated with the 2005 West off Fukuoka Prefecture Earthquake Derived from ENVISAT/InSAR and Fault-slip Modeling

Report of the National Research Institute for Earth Science and Disaster Prevention, No. 69 ; August, 2006

Crustal Deformation Associated with the 2005 West Off Fukuoka Prefecture Earthquake Derived from ENVISAT/InSAR and Fault-slip Modeling

Taku OZAWA*, Sou NISHIMURA**, and Hiroshi OHKURA*

*Volcano Research Department,
National Research Institute for Earth Science and Disaster Prevention, Japan
taku@bosai.go.jp, ohkura@bosai.go.jp
**Earthquake Research Department,
National Research Institute for Earth Science and Disaster Prevention, Japan
yeti@bosai.go.jp

Abstract

A shallow M7.0 earthquake occurred off-shore to the west of Fukuoka City in northern Kyushu district, Japan, on March 20, 2005. We attempted to apply ENVISAT/InSAR to detect spatially detailed crustal deformation associated with this earthquake. A displacement of -8cm in the line-of-sight component was found on the Itoshima Peninsula located to the south of the fault, and one of +5cm was found in an east area of the fault. The displacements obtained from InSAR analysis corresponded to within 1cm of those from GEONET. This pattern corresponded roughly with crustal deformation induced by a left-lateral fault slip directed to the west-northwest that was suggested from seismic data. We attempted to estimate a fault-slip distribution by inverting crustal deformations obtained from InSAR and GEONET, and an asperity related to this earthquake was found at a shallow depth just above the hypocenter of the mainshock. Around the hypocenter of the largest aftershock that occurred after SAR observations, the left-lateral fault slip was insignificant. This suggests that the largest aftershock occurred in the locked area, not in the area where a fault rupture had occurred.

Key words : The 2005 West Off Fukuoka Prefecture Earthquake, InSAR, ENVISAT, Coseismic deformation, Fault slip model

1. Introduction

On March 20, 2005, a shallow earthquake (M_{JMA}=7.0) occurred off-shore to the west of Fukuoka City, in northern Kyushu, Japan. According to the Japan Meteorological Agency (JMA), the hypocenter of this earthquake was located at 33.739°N latitude, 130.176°E longitude, at a depth of 9.2km (**Fig.1**(**a**)), and the focal mechanism was a lateral strike slip fault type. Aftershocks aligned along a near-vertical and west-northwest striking plane similar to one of the mainshock nodal planes (**Figs.1**(**a**) and (**b**)), indicating that this earthquake was induced by a left-lateral strike slip on a fault plane directed to the west-northwest. The largest aftershock (M_{JMA}=5.8) occurred around the east-southeast end of the aftershock distribution on April 20, and its focal mechanism was similar type to that of the mainshock (**Fig.1**(**a**)).

Crustal deformation associated with this earthquake was observed by the Japanese nationwide GPS array named GEONET (Sagiya *et al*., 2000). It demonstrated that GPS sites located to the east and south of the fault had moved to the west and south due to the earthquake (**Fig.2**). Such a pattern can be roughly explained by crustal deformation that was induced by the fault mechanism suggested from seismic data. To investigate the fault mechanism in more detail, spatially denser crustal deformation data was needed. Thus, we applied the interferometric synthetic aperture radar technique (InSAR) and succeeded in obtaining more crustal deformation data. Additionally, we attempted to model the fault-slip distribution using InSAR and GEONET data. In this paper, we present coseismic deformation obtained from InSAR analysis and the

* Tennodai 3-1, Tsukuba, Ibaraki, 305-0006, Japan
** Tennodai 3-1, Tsukuba, Ibaraki, 305-0006, Japan

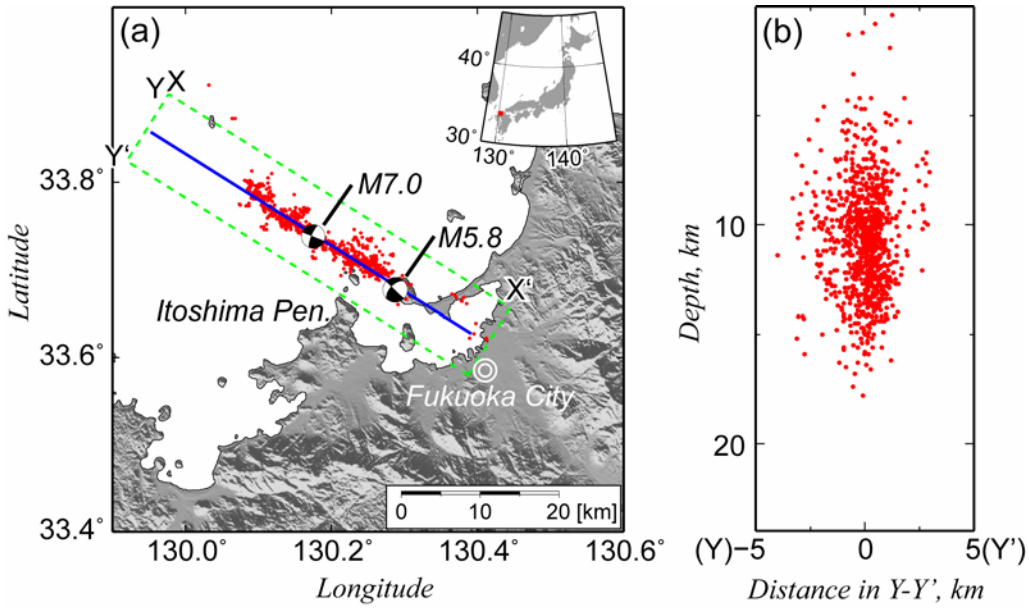

Fig.1 (a) Shaded-relief topographic map around the study area. Depicted focal mechanisms of the mainshock (M7.0) and the largest aftershock (M5.8) were provided by the Japan Meteorological Agency (JMA). Red dots indicate the distribution of the aftershocks (M≥2) that occurred from March 20 to March 30 as provided by JMA. Aftershocks that occurred in the broken green rectangle were used to prepare **Fig.1**(**b**) and **Fig.4**. The thick blue line indicates the fault location defined from aftershock distribution. The inset shows the area of this figure. (b) Aftershock distribution projected onto Y-Y' of **Fig.1**(**a**).

fault-slip distribution that was estimated from InSAR and GEONET data.

2. ENVISAT/InSAR data

In this InSAR analysis, we used ENVISAT SAR data acquired from descending orbits on February 23 (master image) and March 30 (slave image). The observation mode was "IS2"; the incidence angle was 23°, the swath width was 100km, and the pixel sizes were 8 and 4 meters in the range and azimuth directions. The line-of-sight (LOS) direction of the radar in these observations was (-0.3772, 0.0899, -0.9217) in the coordinate set (east, north, up). InSAR can detect one component of which a displacement vector projected onto the LOS direction. Crustal deformation that can be obtained from this InSAR pair is mainly due to the mainshock. Although an M5.4 aftershock occurred on March 22, its contribution to crustal deformation was small.

Fig.3(**a**) presents the obtained interferogram. Each fringe on the interferogram (one color cycle: blue-purple-yellow-blue) is consistent with an LOS displacement of 2.8cm, half of the wavelength of the radar. The difference of satellite positions observed in the master and slave images was 380m, indicating that the application condition of InSAR was acceptable. Therefore a good coherence was obtained especially in the populated area, but coherence in the mountain area was low. It must have

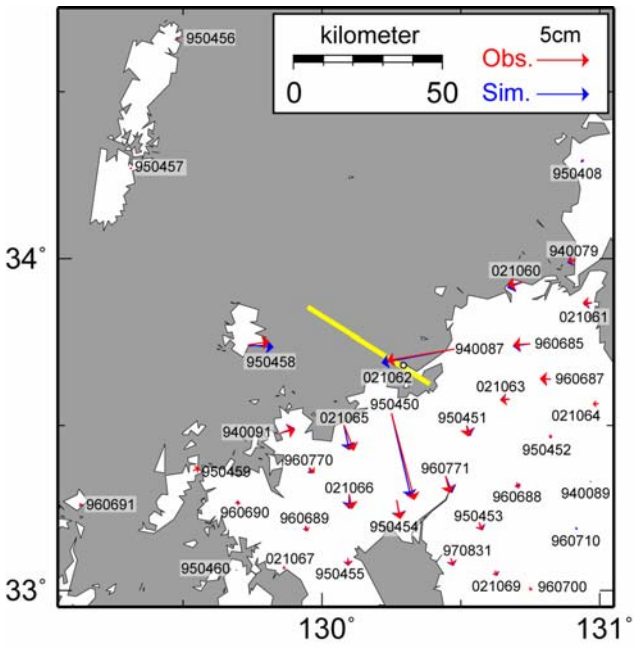

Fig.2 Horizontal displacement vectors at the GEONET sites. Red and blue arrows indicate the observed and simulated displacements. The yellow line corresponds to the blue line of **Fig.1**(**a**). Site number of GEONET site is attached to each arrow.

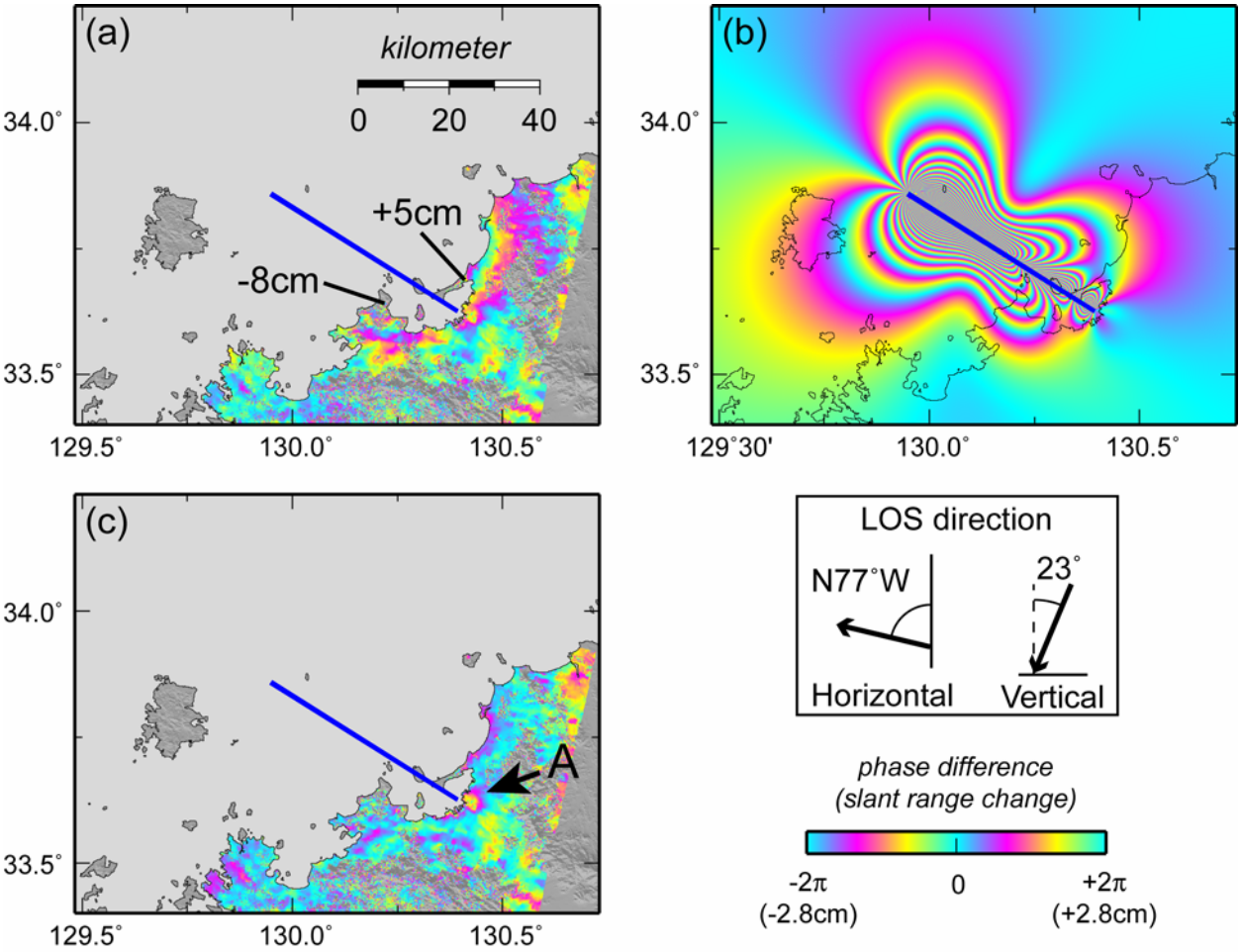

Fig.3 (a) Observed interferogram. Color bar shows a phase difference from –2π to +2π radian. A phase difference of 2π radian corresponds with a displacement of 2.8cm in the line-of-sight (LOS) direction component. The LOS direction is shown above the color bar. The blue line corresponds to the blue line of **Fig.1**(**a**). (b) Simulated interferogram. (c) Residual interferogram (observation – simulation).

been due to a temporal decorrelation related to vegetation (Zebker and Villasenor, 1992).

In the coastal area neighboring the seismic area, the characteristic fringe pattern was detected. It indicated that the eastern area of the fault moved away from the satellite. In the northern part of Fukuoka City, a displacement exceeding +5cm in the LOS component was detected (**Fig.3**(**a**)). In contrast, crustal deformation that moved toward the satellite was found in the south of the fault, and a displacement of -8cm in the LOS component was detected on the Itoshima Peninsula (**Fig.3**(**a**)). Such a pattern can also be explained by crustal deformation that was induced by a fault mechanism suggested from seismic data. Although InSAR can detect crustal deformation only in a land area, it is estimated that a larger displacement had occurred near the fault located in an ocean area.

To validate displacements obtained from InSAR analysis, we compared them with the LOS component of displacement that was calculated from GEONET F2

Table 1 Comparison between InSAR and GPS displacements in the LOS component.

Station No.	InSAR[mm]	GPS[mm]	Res.[mm]
940087	23	27	-4
940091	1	-8	9
950450	-9	-19	10
950451	-4	0	-4
950454	1	-2	3
950455	-4	-6	2
950459	-1	-4	3
960689	-2	-1	-1
960690	-4	0	-4
960770	-5	-2	-3
960771	-1	-3	2
970831	-5	-2	-3
021060	-8	2	-10
021066	1	2	-1
021067	1	1	0

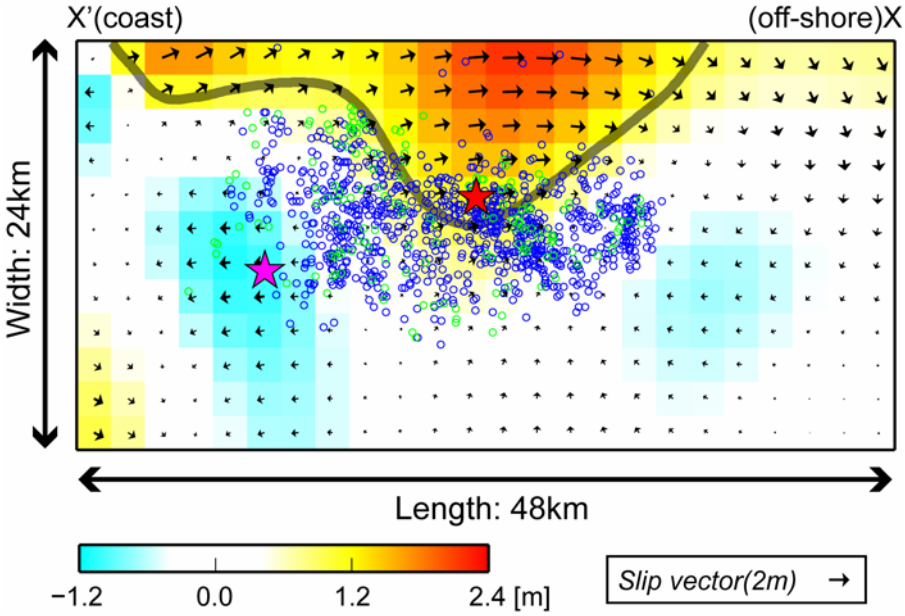

Fig.4 Estimated fault-slip distribution. Color bar shows a strike slip from -1.2m to 2.4m (a plus is a left-lateral strike slip). Segment size is 2×2km. Red and purple stars indicate the locations of hypocenters of the mainshock and the largest aftershock that were projected onto the fault (X-X' of **Fig.1**(**a**)), and blue circles indicate those of other aftershocks (M≥2) that occurred before SAR observation time of the slave image. Green circles indicate those of aftershocks that occurred from SAR observation time of the slave image until the occurrence time of the largest aftershock. The transparent thick curve indicates a 1-m contour for the strike slip.

analysis data (**Table 1**). Displacements of GEONET were calculated from the difference of averaged positions over 11 days centered on February 23 and March 30, the observation dates of the master and slave images. The maximum disagreement was 10mm and the standard deviation of the residual was 5mm. This indicated that one cycle of a phase difference that was a displacement of 28mm in the LOS component was sufficiently significant.

3. Modeling of fault slip distribution

Using crustal deformation data that were obtained from InSAR and GEONET, we attempted to estimate the fault-slip distribution by inversion analysis of the elastic-half space dislocation theory (Okada, 1985). There were InSAR displacement data at 380,000 points, so it would have been inefficient to input all data points into the inversion analysis. Instead, the Quadtree algorithm (Samet and Webber, 1988), which averages displacement data in an adaptive spatial size, was applied, and the amount of InSAR data was reduced to 255 points. The GEONET data were the horizontal components at 35 sites that were located between 129° and 131° longitude and between 33° and 35° latitude. Displacement at the GEONET site "021062" was excluded, because it was located just above the fault, and there was a possibility that its displacement could not be explained by an elastic theory.

The strike and dip directions of the fault were defined as 302° and 90°, which were determined from aftershock distribution by the JMA earthquake catalogue (**Figs.1**(**a**) and (**b**)). The length and width of the fault were set to 48 and 24km, which is sufficiently large relative to the aftershock distribution. This area was divided into 2 by 2km fault segments, and the fault-slip vector at each segment was estimated by inversion analysis. In this analysis, only a smoothness constraint by the Laplacian of the fault-slip distribution was used to stabilize the results, and the strength of the constraint was determined so that Akaike's Basian Information Criterion (ABIC) was minimized (Akaike, 1980).

4. Result and Discussion

Fig.4 illustrates the distribution of the estimated fault slip, which revealed that a lateral-strike slip was dominant in the whole fault. In particular, a large left-lateral strike slip of more than 1m was found in the area shallower than 10km depth around the center of the fault, and its area extended toward the coastal area only at a depth of up to 4km depth. The GEONET displacements that were simulated from such fault-slip distribution explained

observed ones well (**Fig.2**). The root-mean squared residual (RMS) was 2mm. Simulated InSAR displacements also explained observed ones well (**Figs.3**(**b**) and (**c**)). The RMS was 6mm, corresponding to the standard deviation of residuals between InSAR and GEONET data. A grained pattern of a fringe with an amplitude of a half cycle remains in the whole image (**Fig.3**(**c**)), but we think that this is noise caused by an atmospheric effect (*e.g.* Goldstein, 1995). Except for an area close to the fault, such noise cannot largely affect the estimation of fault-slip distribution because it has a wavelength of several kilometers, which is sufficiently small relative to that of crustal deformation caused by the faulting. A fringe pattern with a phase difference of one cycle remains around the southeast end of the fault, suggesting an actual surface deformation (A in **Fig.3**(**c**)). This fringe pattern, however, cannot be explained by crustal deformation that was induced by a fault slip on a vertical fault because it should induce negative fringe patterns on each side of the fault. Conceivably, this deformation might be land subsidence that was caused by the earthquake. A right-lateral strike slip that estimated in the shallow part of the southeast end of the fault may be an artifact that was caused by this deformation pattern.

To investigate the relation between fault-slip distribution and aftershock distribution, hypocenters of aftershocks with magnitudes of more than 2 that occurred during SAR observation period were projected onto the fault plane (blue circles in **Fig.4**). The red star represents the location of the mainshock. A large left-lateral strike slip of more than 2m was found just above the hypocenter of the mainshock, indicating an asperity related with this earthquake. Aftershocks occurred in the width of 8km surrounding this asperity, and its area had barely exceeded the area where a slip of 1m was found (the transparent thick curve in **Fig.4**). This suggests that stress that had been accumulated in the asperity was completely released at the mainshock, and that aftershocks occurred in the area where stress had not been released completely or where stress was increased by its reallocation. On the other hand, a small right-lateral fault slip was estimated around the hypocenter of the largest aftershock that occurred on April 20 (the purple star of **Fig.4**). Although this may be an artifact of the analysis, at least the fault rupture must have been insignificant during the SAR observation. Moreover aftershocks had scarcely occurred until April 20 in this area (blue and green circles of **Fig.4**). These facts suggest that the largest aftershock occurred in the locked area, not in the area where a fault rupture had occurred.

5. Conclusions

We applied InSAR using ENVISAT data to detect crustal deformation associated with the 2005 West Off Fukuoka Prefecture Earthquake, and obtained a result that was consistent with other observations. Inverting obtained crustal deformations with GEONET data, we found an asperity of this earthquake in a shallow depth just above the hypocenter of the mainshock. Furthermore the estimated fault-slip model suggests that the largest aftershock on April 20 occurred in a locked area, not in the area where a fault rupture had occurred.

Acknowledgements

We thank H. Ueda (NIED) for a careful reading of the manuscript. The hypocentral data was provided by the Japan Meteorological Agency in cooperation with the Ministry of Education, Culture, Sports, Science, and Technology. The coordinate data of GEONET F2 analysis was provided by the Geographical Survey Institute of Japan. The copyright of the original ENVISAT SAR data own by the European Space Agency, and data were distributed by Eurimage. All figures were drawn using the Generic Mapping Tools from Wessel and Smith (1998).

References

1) Akaike, H. (1980): Likelihood and Bayes procedure, in Baysian Statistics, edited by J. M. Bernardo *et al*., pp. 143-166, Univ. Press, Valencia, Spain.
2) Goldstein, R. (1995): Atmospheric limitations to repeat-track radar interferometry, Geophys. Res. Lett., **22**-18, 2517-2520.
3) Okada, Y. (1985): Surface deformation due to shear and tensile faults in a half-space, Bull. Seism. Soc. Am., **75**, 1135-1154.
4) Sagiya, T., Miyazaki, S., and Tada, T. (2000): Continuous GPS array and present-day crustal deformation of Japan, PAGEOPH, **157**, 2303-2322.
5) Samet, H. and Webber, R. E. (1988): Hierarchical data structures and algorithms for computer graphics. I. Fundamentals, IEEE Comput. Graphics Appl., **8**-3, 48-68.
6) Wessel, P. and Smith, W. H. F. (1998): New improved version of generic mapping tolls released, EOS Trans. AGU, **79**-47, 579.
7) Zebker, H. A. and Villasenor, J. (1992): Decorrelation in interferometric radar echoes, IEEE Trans. Geosci. Remote Sensing, **30**, 950-959.

(Accepted : May 23, 2006)

ENVISAT/InSAR によって捉えられた 2005 年福岡県西方沖の地震に伴う地殻変動および断層すべり分布の推定

小澤　拓[*]・西村　宗[**]・大倉　博[*]

[*]独立行政法人　防災科学技術研究所　火山防災研究部
[**]独立行政法人　防災科学技術研究所　地震研究部

要　旨

2005 年 3 月 20 日に福岡県西方沖において発生した地震（M_{JMA}=7.0）に伴う地殻変動を検出するために，ENVISAT 衛星を利用した SAR 干渉法の適用を試みた．断層の南に位置する糸島半島においては，人工衛星と地表との距離（スラントレンジ）が 8cm 短縮する地殻変動が観測され，断層の東方域においてはスラントレンジが 5cm 伸張する地殻変動が観測された．このような地殻変動パターンは，西北西－東南東方向に走向を持つ断層の左横ずれを考慮することによって説明することが可能である．これは地震観測データ等から示唆される結果と調和的である．また，SAR 干渉法により得られた地殻変動は，国土地理院による GPS 観測網（GEONET）によって観測された地殻変動と 1cm 以内で一致することから，精度良く地殻変動が検出できたといえる．そこで，SAR 干渉法と GEONET から得られた地殻変動データを用いて，断層内のすべり分布を推定したところ，本震の震源直上において大きな左横ずれが求められた．一方，SAR 観測以降に発生した最大余震の震源周辺においては，有意な大きさのすべりは求められなかった．このことは，最大余震は固着していた領域において発生したことが示唆される．

キーワード：2005 年福岡県西方沖地震，SAR 干渉法，地殻変動，断層すべり分布